Serum starvation in HT-22 mouse hippocampal cells leads to the hyperpolarization of the mitochondrial membrane potential

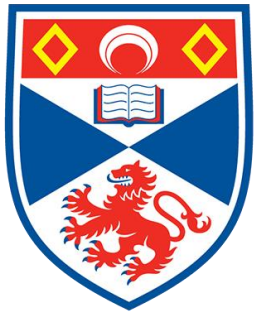

University of
St Andrews

Aleksandra Tracichleb

at336

Supervised by Dr Gayle Doherty

School of Psychology and Neuroscience

Table of Contents

Serum starvation in HT-22 mouse hippocampal cells leads to the hyperpolarization of the mitochondrial membrane potential

1. Introduction:

The vital importance of mitochondrial function is striking in neurons, which display significantly higher energy demand than the rest of the tissues (Allen *et al.*, 2018). These organelles are not only the main place of adenosine triphosphate (ATP) production through oxidative phosphorylation but are also crucial for Ca^{2+} homeostasis within the cell. Hence, neurons are highly vulnerable to any impairments in mitochondrial functioning and subsequent impairments in energy production, which lead to imbalance in neurotransmitter release, Ca^{2+} equilibrium, neuroplasticity, and inflammatory response (Chen *et al.*, 2024). All these impairments were shown to be involved in the development of many neurodegenerative and neurodevelopmental diseases such as Alzheimer's disease (AD) and Parkinson's disease (PD).

Measuring the mitochondrial membrane potential ($\Delta\psi_m$) is crucial in assessing mitochondrial functioning and viability and its fluctuations are linked to cellular dysfunctions (Carrageta *et al.*, 2022; Zorova *et al.*, 2018). $\Delta\psi_m$, described as the electrical difference between the mitochondrial matrix and cytosol, is maintained by properly functioning proton pumps in the mitochondrial electron transport chain (Aldana *et al.*, 2021; Shao *et al.*, 2018). Due to its critical importance in ATP production, fluctuations beyond the norm often result in cellular disruptions. The decrease in $\Delta\psi_m$ usually indicates impairments in bioenergetic balance and

can result in the release of apoptotic molecules, whereas a sudden increase in $\Delta\psi_m$ indicates higher rates of reactive oxygen species formation (Li *et al.*, 2022; Gutiérrez *et al*., 2017).

The effects of the serum starvation were investigated on the immortalised mouse HT-22 hippocampal cell culture, which is used as a research model for research in cognitive functions impairment and AD (Lim *et al*., 2023). To assess the effects of stress induced by serum starvation, the fluorescent 5,5',6,6'-tetrachloro-1,1',3,3'-tetraethylbenzimidazolylcarbocyanine (JC-1) dye was used. JC-1 can accurately assess the $\Delta\psi_m$ in both healthy and apoptotic cells due to its varying fluorescent emissions in differing $\Delta\psi_m$. Naturally, JC-1 exhibits green fluorescence, however, it can enter the mitochondria in healthy cells, forming J-aggregates, which exhibit red fluorescence (Sivandzade *et al.*, 2019). Therefore, in healthy cells with normal $\Delta\psi_m$ JC-1 will exhibit red fluorescence, whereas the green fluorescence will be retained by JC-1 in the decreased $\Delta\psi_m$ in apoptotic cells. Therefore, in this study, the red-to-green fluorescence ratio was used to assess mitochondrial well-being and viability.

Moreover, two different concentrations of leptin were used to investigate its effect on $\Delta\psi_m$ in serum-starved cells. Leptin is a hormone derived from adipose tissue, with an important role in the hypothalamic regulation of food intake and fat storage. Moreover, it was also demonstrated to have a central role in neural differentiation and maintenance of neuronal stem cells (Tan *et al.*, 2023). These neuroprotective effects extend to the models of neurodegenerative diseases, such as AD, showing a strong link between increased neuronal survival and improved mitochondrial functioning (Cheng *et al.*, 2020). Therefore, this study investigated the effects of leptin on the mitochondrial $\Delta\psi_m$ to explore the mechanism of its neuroprotective properties.

Lastly, to further assess the mitochondrial role in cellular functioning, the mitochondrial dynamics were assessed in the rat cells from enriched and standard environments. The Fis1 and Mfn1 mitochondrial fission and fusion protein levels were investigated using Bradford assays and the enzyme-linked immunosorbent (ELISA) assays. Bradford was used to assess the initial levels of proteins in each of the samples whereas ELISA was used to establish the exact levels of Mitochondrial Fission Protein 1 (Fis1) and Mitochondrial Fusion Protein 1 (Mfn1). Assessing the link between environmental enrichment and mitochondrial dynamics will provide insight into the underlying mechanisms of neuroprotective properties of enriched environments, investigating if observed difference arises due to the differing levels of fission and fusion proteins.

1.1. Hypothesis

It is hypothesized that the use of leptin in serum-starved HT-22 cells will result in inhibition of $\Delta\psi_m$ decrease after 2, 4 and 6 hours of serum withdrawal due to its neuroprotective properties. Moreover, based on the existing literature it is speculated that enriched environment will result in lower levels of Fis1 and higher levels of Mfn1 compared to the standard environment condition (Deng et al. 2022).

2. Methods:

2.1. JC-1 mitochondrial staining:

HT-22 mouse hippocampal cell line was cultured in 20% FCS medium (Dulbecco's modified eagle medium), which contained 20% (v/v) iron-fortified fetal bovine calf serum, 4.5 g/l D-glucose, 10 mg/m penicillin/streptomycin. The cells were counted using a hemocytometer and seeded at a density of $1*10^4$ on a 96-well culture plate. Four different groups of cells were present: the control group G, consisting of the HT-22 cells with serum, group F with serum withdrawn, group E with serum withdrawn and 1nM of leptin treatment and group D with withdrawn serum and 10nM of leptin treatment. All treatments and controls were carried out in 12 replicates.

Then, the cells were incubated for 2, 4 and 6 hours. After the incubation period, all the medium was removed, and the samples were washed with room-temperature phosphate buffered saline (PBS). After washing, fresh PBS and the 10µg JC-1 dye at the concentration of 1mg/1ml were added to all the wells, including the controls. The samples were incubated for 45 minutes, after which the medium was removed. The samples were washed in PBS, after which fresh PBS was added. The plates were covered with the tin foil until placed on the plate reader to avoid JC-1 photobleaching. The red fluorescence was measured first, as it fades quicker, at the excitation wavelength of 544 nm and emission wavelength of 575 nm. Subsequently, the green fluorescence was measured at the excitation wavelength of 485 nm and emission wavelength of 535 nm.

2.2. Bradford Assay:

In the second experiment, the rats' brain tissues obtained from Prof. James Ainge's lab were used. The brain tissues obtained from animals 1, 3, 4, 5, 7, 9, 10, 11, 15, 17, 18, 19, 20, 21 were used in Bradford and ELISA.

The initial protein concentration in all samples was assessed by conducting Bradford assays. Firstly, all the samples were homogenised in a lysis buffer to ensure uniform distribution of proteins across the sample. Next, a 10-fold serial dilution of bovine serum albumin (BSA), with concentration rage of 10mg/ml, 1mg/ml, 100µg/ml, 10µg/ml and 1µg/ml, was prepared by dilution in *d*H2O to form a standard curve. Then, 10 µl of the sample was mixed with 10µl of 1M NaOH, which allowed for membrane solubilization and systematised colour variation between proteins (Stoscheck, 1990). The negative controls were prepared by mixing 10 µl of lysis buffer with 10µl of 1M of NaOH. Next, the 500 µl of Bradfordt reagent (50 mg Brilliant Blue stain, 50ml methanol, 100ml 85% Phosphoric Acid, and 850 ml H_2O) was added to each of the samples to assess their protein levels. The 100µl of each sample was subsequently transferred onto the Bradford plate in triplicate and covered with tin foil as Bradford reagent is photosensitive. After 5 minutes the absorbance was read at 570 nm and recorded.

2.3. Enzyme-linked Immunosorbent Assay:

ELISA assays were conducted on a microplate 96-well F-bottom ELISA high binding plate. Primary mouse monoclonal antibody Mfn1, primary monoclonal rabbit antibody Fis1 and alpha tubulin were diluted with three dilution factors: 1:20, 1:200 and 1:2000. The secondary antibodies of HRP-conjugated anti-mouse and HRP-conjugated anti-rabbit were used at the dilution factor of 1:10,000. The stock solutions were made of homogenized rat brain tissues and Tris-buffered saline (TBS) buffer. Next, they were transferred to the Eppendorfs, vortexed and denatured in 90°C water for 10 minutes. Subsequently, 50 µl of each solution was added to wells in triplicate. Three negative controls, containing the same solution as the treatment conditions, and three negative controls containing the extraction solution were added at the volume of 50 µl per well. The ELISA plates were placed on the rocker for 2

hours and were incubated overnight at 4°C.

Next day, the liquid from the wells was removed and 200µl of 5% milk serum (2.5 g. Marvel milk powder, 47.5 ml TBS-T) was added to each well to block the non-specific antibody binding. The samples were incubated on the rocker for 2 hours at room temperature, with cover to prevent drying of the wells. Then, the 5% milk serum was pipetted out three wells at a time and the 100µl of Alpha-tubulin, Mnf1 and Fis1 primary antibody solutions were added to each well, except the controls. The 100 µl of 1% milk serum in TBS was added to all negative controls. The plate was covered to avoid wells drying out, placed on the rocker for 2 hours and then incubated overnight in the 4°C.

On the third day, the primary antibody solutions and 1% milk serum (3 ml 5% milk solution, 12 ml TBS-T) were removed, and the wells were washed in the 200 µl of the TBS solution and incubated for 10 minutes on the rocker, covered. The procedure was repeated three times. The 50 µl/well of the secondary antibody was added to all the wells, including the controls. The HRP-conjugated anti-mouse was used as a secondary antibody for Mfn1 and Alpha tubulin whereas the HRP-conjugated anti-rabbit was used as a secondary antibody for Fis1. The plate was incubated on a rocker with a cover in the room temperature for an hour. After the incubation period, the secondary antibodies were removed and all the wells were washed three times in the TBS buffer, with 10-minute incubation periods on a rocker in between every wash. Then, the TBS buffer was removed and 3,3',5,5'-Tetramethylbenzidine (TMB) substrate was added to all the wells. The plate was covered with tin foil to avoid TMB photobleaching and the sample was left to develop blue colour. After the colour emerged or after 25 minutes, the reaction was stopped by adding 100µl of 0.1M of HCl. The absorbance values were read with the plate reader at 490 nm and the results were recorded.

2.4. Statistical Analysis

The statistical analysis was performed using JASP. The normality of data was assessed using Q-Q plots and homogeneity of variance using Levene's test. As all the assumptions for the parametric test were met, the one-way analysis of variance (ANOVA) test was conducted. A p value lower than 0.05 was considered as statistically significant.

3. Results:

In this experiment the assays with the fluorescent JC-1 dye were conducted to assess the viability and well-being of the serum-stressed HT-22 cells by assessing their $\Delta\psi_m$. The effects of serum withdrawal duration and leptin were investigated. Hence, the difference in $\Delta\psi_m$ between 2, 4 and 6 hours from serum withdrawal was assessed, as well as the difference between the controls and treatments with 1nM and 10nM of leptin. As all the requirements for the parametric test were met, the one-way ANOVA analysis was used for all the statistical analysis.

3.1. 6-hour serum withdrawal results in higher red-to-green fluorescent ratio than 2- and 4- hours withdrawal periods

The Bonferroni-corrected post-hoc pairwise contrast revealed that there was a significant difference in red-to-green fluorescence between the 2-hour condition ($M = 0.644$, $SD = 0.095$) and 6 hour condition ($M = 0.764$, $SD = 0.063$) ($p<0.001$), and between 4-hour condition ($M = 0.630$, $SD = 0.086$) and 6-hour condition ($M = 0.764$, $SD = 0.063$) ($p<0.001$)

(see Fig.1). There was no significant difference between the 2-hour condition (M = 0.644, SD = 0.095) and 4-hour condition (M = 0.630, SD = 0.086).

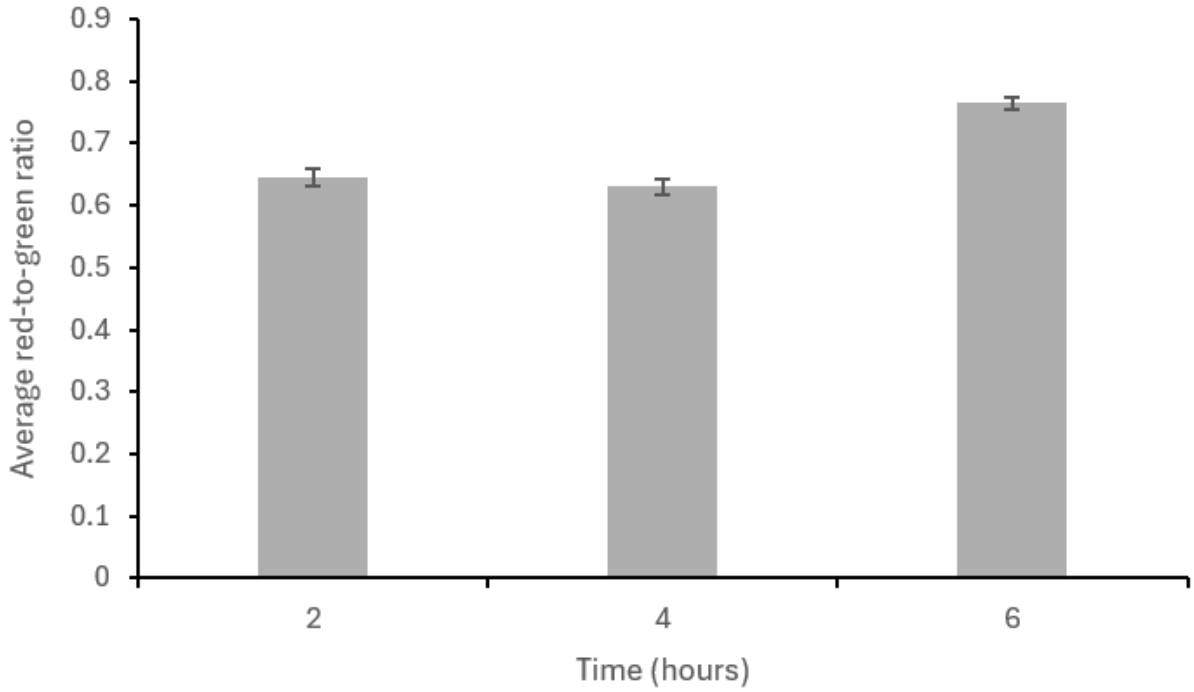

Fig. 1: Average red-to-green fluorescence ratio against time. *The mean red-to-green fluorescence ratio stayed on the same level from 2 to 4 hours of serum deprivation. Then, the mean red-to-green fluorescence ratio increased from 4 to 6 hours of serum deprivation. Error bars represent standard error.*

3.2. There is no significant difference in red-to-green fluorescence ratio between leptin treatments and the controls

To investigate if leptin exerts its neuroprotective properties via changes in $\Delta\psi_m$ the red-to-green fluorescence ratio was calculated for 2-, 4-, and 6-hour withdrawal periods. HT-22 cells were treated with: no treatment with serum, no serum, no serum + 1nM of leptin and no serum and 10nM of leptin (see Fig. 2). The Bonferroni-corrected post-hoc pairwise contrast

revealed that there was no significant difference in red-to-green fluorescence ratio between any of the conditions 2 hours after the serum withdrawal.

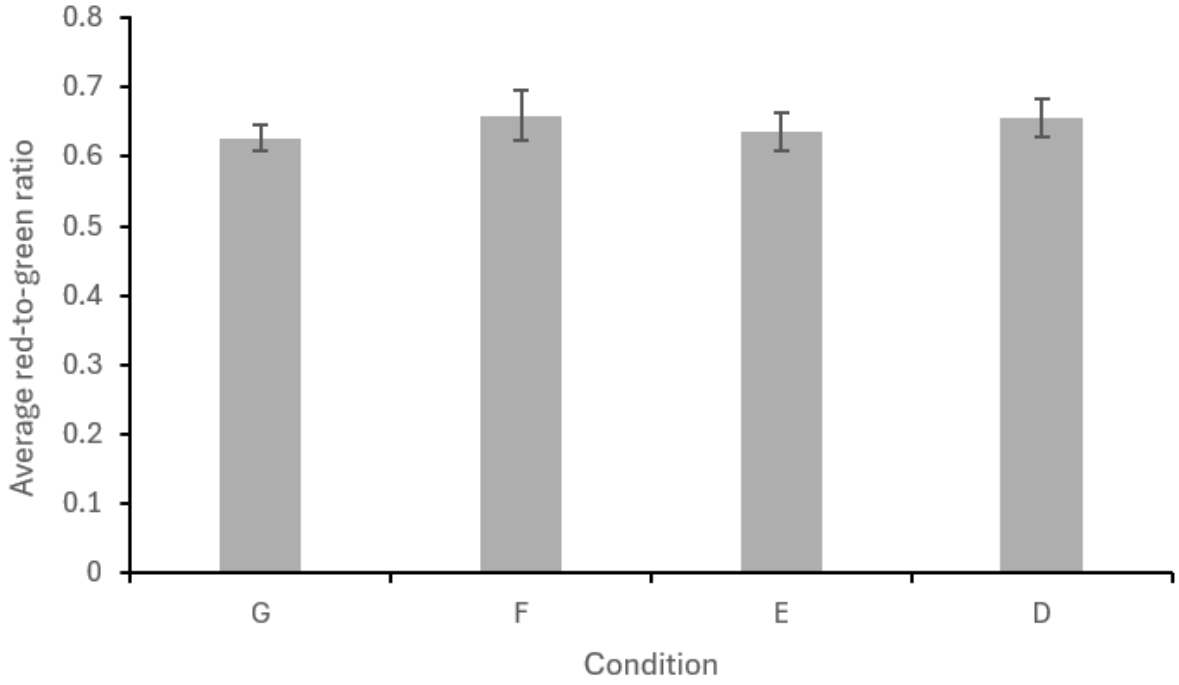

Fig. 2: Average red-to-green fluorescence ratio across different conditions after 2 hours of serum starvation. *(G) control containing HT-22 cells and serum. (F) treatment condition with HT-22 cells and withdrawn serum. (E) treatment condition with HT-22 cells, withdrawn serum and 1nM leptin. (D) treatment condition with HT-22 cells, withdrawn serum and 10nM leptin. The error bars represent standard error.*

There was no also significant difference in red-to-green fluorescence ratio according to Bonferroni-corrected post hoc pairwise contrast between any of the conditions 4 hours after the serum withdrawal (see Fig. 3).

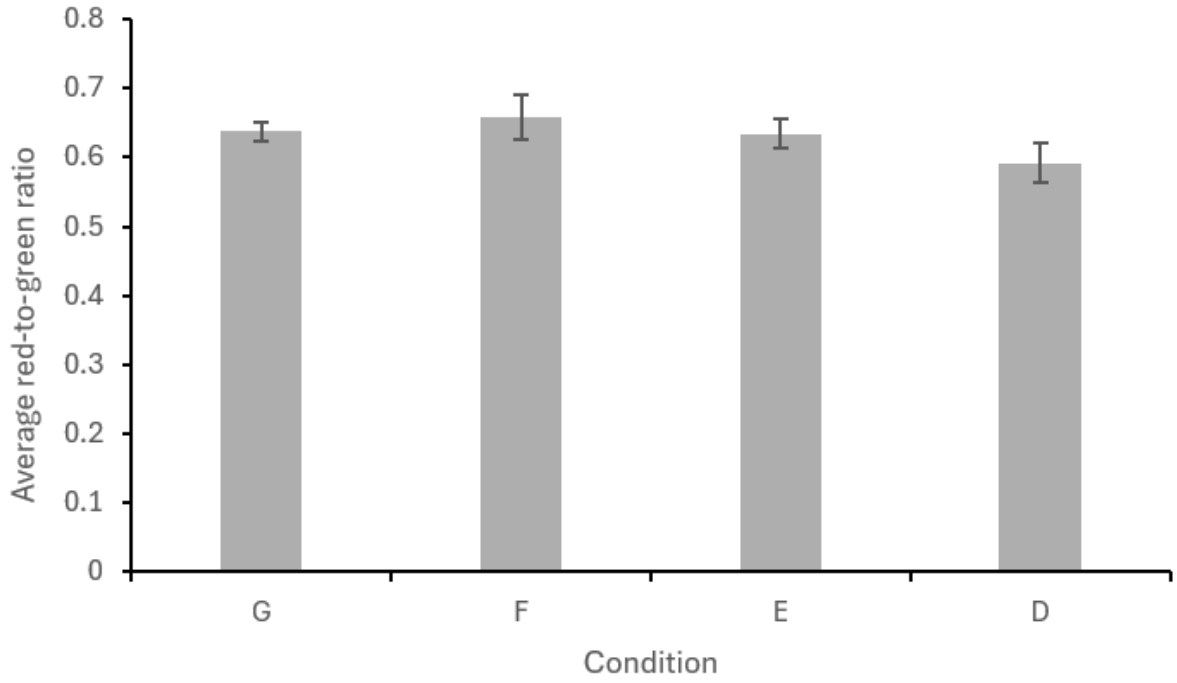

Fig. 3: Average red-to-green fluorescence ratio across different conditions after 4 hours of serum starvation. *(G) control containing HT-22 cells and serum. (F) treatment condition with HT-22 cells and withdrawn serum. (E) treatment condition with HT-22 cells, withdrawn serum and 1nM leptin. (D) treatment condition with HT-22 cells, withdrawn serum and 10nM leptin. The error bars represent standard error.*

Lastly, there was no significant difference in red-to-green fluorescence ratio according to Bonferroni-corrected post hoc pairwise contrast between any of the conditions 6 hours after the serum withdrawal (see Fig. 4).

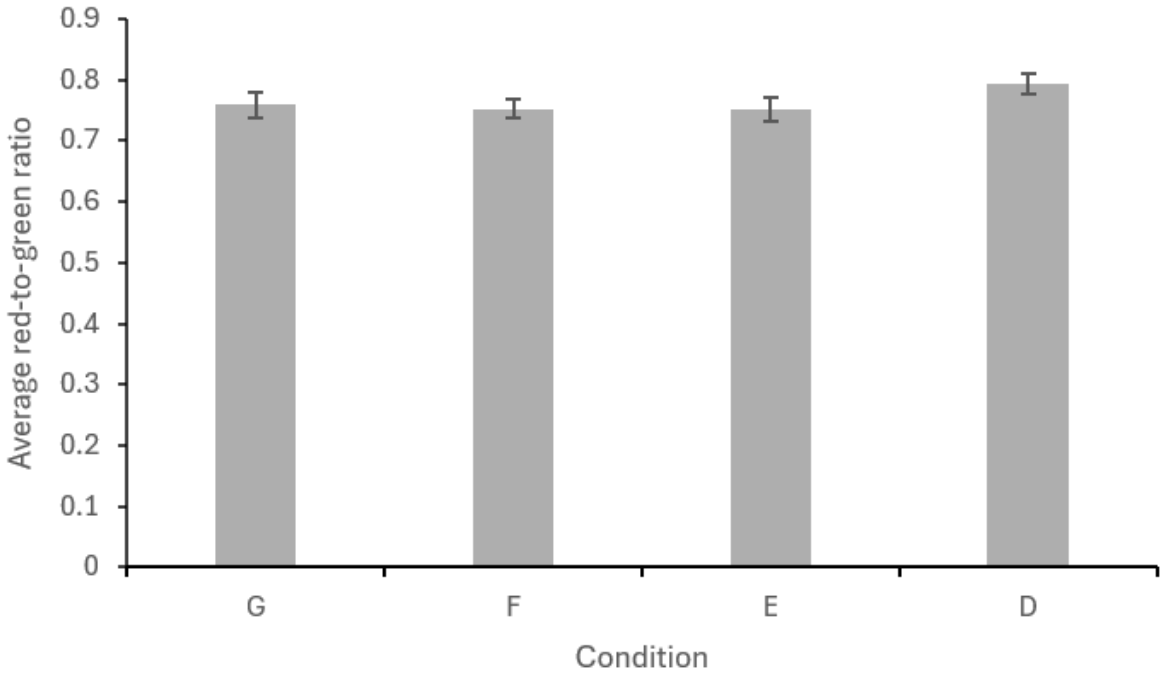

Fig. 4: Average red-to-green fluorescence ratio across different conditions after 6 hours of serum starvation. *(G) control containing HT-22 cells and serum. (F) treatment condition with HT-22 cells and withdrawn serum. (E) treatment condition with HT-22 cells, withdrawn serum and 1nM leptin. (D) treatment condition with HT-22 cells, withdrawn serum and 10nM leptin. The error bars represent standard error.*

4. Discussion:

The experiment investigated the effect of serum withdrawal and different leptin concentrations (1nM and 10nm) on $\Delta\psi_m$ in HT-22 mouse hippocampal cells. The results revealed that leptin didn't have any significant effect on the $\Delta\psi_m$. It was also demonstrated that the serum withdrawal time of 6 hours resulted in a significant increase in red-to-green fluorescence ratio compared to 2 and 4-hour withdrawal periods, suggesting an increase in $\Delta\psi_m$ after 6 hours from serum withdrawal.

In their paper, Ijima *et al.* demonstrated that hyperpolarization can be an intermediate stage in apoptosis in response to glucose and oxygen withdrawal (2003). In this study, the hippocampal cell cultures deprived of nutrients for 30 minutes demonstrated not only higher $\Delta\psi_m$ but also the release of cytochrome c release, which is an event characteristic of apoptosis. This hyperpolarization event might suggest impairment of the electron transport chain machinery, responsible for preventing fluctuations in $\Delta\psi_m$. However, this study indicates that the hyperpolarization phase occurs shortly after the serum starvation, of around 30 minutes, after which a decrease in $\Delta\psi_m$ takes place. Contrastingly, this experiment demonstrated that hyperpolarization occurs after 6 hours from the point of cell starvation. The observed difference might be due to the difference in the way cellular stress was induced.: Ijima *et al.* study starved the hippocampal cells of oxygen and glucose instead of serum, which might have accelerated the mitochondrial damage.

Moreover, Colombaioni *et al.* demonstrated that serum-deprived cells were displaying apoptotic events such as Bax translocation to the mitochondria followed by cytochrome c release into the cytosol without any change in $\Delta\psi_m$ (2002). These results might indicate that the initiation of apoptosis can involve more than one pathway and doesn't necessarily include a decrease in $\Delta\psi_m$.

On the other hand, previous studies conducted by Wadia *et al.* have shown that stress induced by serum withdrawal in neurons induces lower $\Delta\psi_m$ after 3 hours (1998). It was further demonstrated that these changes were due to the increased levels of intramitochondrial Ca^{2+} levels. Therefore, the contrasting evidence for the effect of nutrient starvation on $\Delta\psi_m$ is observed in the literature. To investigate if the apoptosis has been initiated, other apoptotic

events such as the levels of intracellular calcium, Bax translocation into the mitochondria, and cytochrome c release into the cytoplasm should be investigated alongside changes in $\Delta\psi_m$ after the serum starvation.

Secondly, the investigation didn't demonstrate any significant difference between control treatment and leptin treatments. In their study, Cheng *et al.* showed that leptin exerted its neuroprotective effects on the differentiated HT-22 hippocampal cell cultures deprived of the glucose and serum (OGD) (2020). It was demonstrated that these beneficial effects were underpinned by the regulatory role of leptin in fission and fusion protein expression and inhibition of $\Delta\psi_m$ decrease. These results were further confirmed by Zhang *et al.*, who also demonstrated that neuroprotective effects of leptin are linked to improved mitochondrial function (2020). The increasing leptin concentrations resulted in the increased $\Delta\psi_m$ in the OGD neurons, inhibition of the key apoptotic stimulus, cytochrome c, and inhibition of apoptosis. These findings do not align with the findings of this study, which didn't demonstrate any significant effect of leptin on the $\Delta\psi_m$ of serum-starved neurons. These differences might be due to the concentrations of leptin used in this study. It was demonstrated that leptin exerts the strongest neuroprotective effects at the concentration of 0.1nM, whereas 1nM was the lowest concentration used in this study (Cheng *et al.*, 2020). Therefore, lower leptin concentrations should be used to investigate its effect on the $\Delta\psi_m$.

The second objective of the experiment was to investigate the effects of enriched and standard environments on the fission and fusion proteins in rat hippocampal cells. However, no data was obtained due to the absence of a signal in the ELISA. The lack of signal might have been an effect of the lack of the protease inhibitor added during the homogenization of the cell cultures. During this process proteases, which are enzymes breaking down proteins,

are released (Burden, 2012). Therefore, lack of the inhibition of the proteases resulted in protein degradation, and hence the target proteins were not present and not detected by ELISA. In future studies, the addition of the appropriate protease inhibitor needs to be ensured to obtain accurate ELISA readings.

However, even though part of the results was not obtained due to the factors mentioned above, the research on the involvement of mitochondria in neurodegenerative disorders should be further explored. For instance, it was demonstrated that the main component of neurotic plaques found in AD, Aβ, interacts with mitochondrial fission and fusion proteins, affecting mitochondrial functioning and morphology (Wang et al, 2009). It was found that AD patients have reduced levels of Fis1 and increased levels of Drp1 and Mnf1 in their hippocampi. Moreover, Tau protein, which is a main component in the neurofibrillary tangles found in AD pathology, was also found to negatively affect mitochondria in AD patients (Kopeikina et al, 2011). It was found that the accumulation of neurofibrillary tangles prevents the correct distribution of mitochondria along the neurons, and the possible interaction of Tau with the fission and fusion proteins was proposed (Manczak & Reddy, 2012). Therefore, even though the involvement of mitochondrial dysfunction in pathogenesis of neurodegeneration is undeniable, it is still not established if the mitochondrial damage and dysfunction play primary role in setting off the neurodegenerative cascade or are rather the effects of protein accumulation. Therefore, future studies should further explore the effects of inherited mtDNA mutations on the risk of developing neurodegenerative diseases. It would give insight into the causational relationship between mitochondrial dysfunction and neurodegenerative diseases, and hopefully would offer new opportunities of therapeutic targets.

5. Bibliography:

Aldana, B.I., Salcedo, C., Freude, K.K., Waagepetersen, H.S. (2021). Cellular bioenergetics in human iPSC–derived glutamatergic neurons in health and disease. *Advances in Stem Cell Biology 10*, pp. 205-221. doi: https://doi.org/10.1016/B978-0-12-823884-4.00008-0.

Allen, J., Romay-Tallon, R., Brymer, KJ., Caruncho, HJ., Kalynchuk, LE. (2018). Mitochondria and Mood: Mitochondrial Dysfunction as a Key Player in the Manifestation of Depression. *Front Neurosci 6*(12). doi: 10.3389/fnins.2018.00386.

Burden, D.W. (2012). Guide to the Disruption of Biological Samples – 2012. *Random Primers 12*, pp. 1-25.

Carrageta, DF., Freire-Brito, L., Oliveira, PF., Alves, MG. (2022). Evaluation of Human Spermatozoa Mitochondrial Membrane Potential Using the JC-1 Dye. *Curr Protoc. 9*. doi: 10.1002/cpz1.531.

Chen, H., Lu, M., Lyu, Q., Shi, L., Zhou, C., Li, M., Feng, S., Liang, X., Zhou, X., Ren, L. (2024). Mitochondrial dynamics dysfunction: Unraveling the hidden link to depression. *Biomed Pharmacother 175*(116656). doi: 10.1016/j.biopha.2024.116656.

Cheng, Y., Buchan, M., Vitanova, K., Aitken, L., Gunn-Moore, FJ., Ramsay, RR., Doherty, G. (2020). Neuroprotective actions of leptin facilitated through balancing mitochondrial morphology and improving mitochondrial function. *J Neurochem. 155*(2):191-206. doi: 10.1111/jnc.15003

Colombaioni, L., Colombini, L., Garcia-Gil, M. (2002). Role of mitochondria in serum withdrawal-induced apoptosis of immortalized neuronal precursors. *Brain Res Dev Brain Res. 134*(1-2). doi: 10.1016/s0165-3806(01)00326-1.

Deng, D., Cui, Y., Gan, S., Xie, Z., Cui, S., Cao, K., Wang, S., Shi, G., Yang, L., Bai, S., Shi, Y., Liu, Z., Zhao, J., Zhang, R. (2022). Sinisan alleviates depression-like behaviors by regulating mitochondrial function and synaptic plasticity in maternal separation rats. *Phytomedicine 106*(154395). doi: 10.1016/j.phymed.2022.154395.

Gutiérrez, L., Stepien, G., Gutiérrez, L., Pérez-Hernández, M., Pardo, J., Pardo, J., Grazú, V., de la Fuente, J.M. (2017). Nanotechnology in Drug Discovery and Development. *Comprehensive Medicinal Chemistry III*, pp. 264-295. doi: https://doi.org/10.1016/B978-0-12-409547-2.12292-9.

Iijima, T., Mishima,T., Akagawa, K., Iwao, Y. (2003). Mitochondrial hyperpolarization after transient oxygen-glucose deprivation and subsequent apoptosis in cultured rat hippocampal neurons. *Brain Research 993*(1-2). Doi: https://doi.org/10.1016/j.brainres.2003.09.041

Kopeikina, K.J., Carlson, G.A., Pitstick, R., Ludvigson, A.E., Peters, A., Luebke, JI., Koffie, R.M., Frosch, M.P. *et al.* (2011). Tau accumulation causes mitochondrial distribution deficits in neurons in a mouse model of tauopathy and in human Alzheimer's disease brain. *Am J Pathol 179*(4). doi: 10.1016/j.ajpath.2011.07.004.

Li, Y., Ma, Y., Dang, Q., Fan, X., Han, C., Xu, S., Li, P. (2022). Assessment of mitochondrial dysfunction and implications in cardiovascular disorders. *Life Sciences 306*. doi: https://doi.org/10.1016/j.lfs.2022.120834

Lim, J., Bang, Y., Kim, K.M., Choi, H.J. (2023). Differentiated HT22 cells as a novel model for *in vitro* screening of serotonin reuptake inhibitors. *Front Pharmacol 13*(1062650). doi: 10.3389/fphar.2022.1062650.

M. Poppe, C. Reimertz, H. Düssmann, A.J. Krohn, C.M. Luetjens, D. Böckelmann, A.L. Nieminen, D. Kögel, J.H.L. Prehn (2001). Dissipation of potassium and proton gradients inhibits mitochondrial hyperpolarization and cytochrome c release during neural apoptosis. *J. Neurosci., 21*(13). Doi: https://doi.org/10.1523/JNEUROSCI.21-13-04551.2001

Manczak, M., Reddy, P.H. (2012). Abnormal interaction between the mitochondrial fission protein Drp1 and hyperphosphorylated tau in Alzheimer's disease neurons: implications for mitochondrial dysfunction and neuronal damage. *Hum Mol Genet 21*(11). doi: 10.1093/hmg/dds072.

Shao, Y., Li, X., Wood, J.W., Ma, J. (2018). Mitochondrial dysfunctions, endothelial progenitor cells and diabetic retinopathy. *Journal of Diabetes and its Complications, 32*(10). doi: https://doi.org/10.1016/j.jdiacomp.2018.06.015.

Sivandzade, F., Bhalerao, A., Cucullo, L. (2019). Analysis of the Mitochondrial Membrane Potential Using the Cationic JC-1 Dye as a Sensitive Fluorescent Probe. *Bio Protoc. 9*(1). doi: 10.21769/BioProtoc.3128

Stoscheck CM (1990). Quantitation of protein. *Methods Enzymol. 182*, pp. 50-68. doi: 10.1016/0076-6879(90)82008-p

Tan, R., Hu, X., Wang, X., Sun, M., Cai, Z., Zhang, Z., Fu, Y., Chen, X., An, J., Lu, H. (2023). Leptin Promotes the Proliferation and Neuronal Differentiation of Neural Stem Cells through the Cooperative Action of MAPK/ERK1/2, JAK2/STAT3 and PI3K/AKT Signaling Pathways. *Int J Mol Sci. 24*(20). doi: 10.3390/ijms242015151.

Wadia, JS., Chalmers-Redman, RM., Ju, WJ., Carlile, GW., Phillips, JL., Fraser, AD., Tatton, WG. (1998). Mitochondrial membrane potential and nuclear changes in apoptosis caused by serum and nerve growth factor withdrawal: time course and modification by (-)-deprenyl. J *Neurosci. 18*(3). doi: 10.1523/JNEUROSCI.18-03-00932.1998.

Wang, X., Su, B., Lee, HG., Li, X., Perry, G., Smith, MA., Zhu, X. (2009). Impaired balance of mitochondrial fission and fusion in Alzheimer's disease. *J Neurosci 29*(28). doi:10.1523/JNEUROSCI.1357-09.2009.

Zhang, W., Jin, Y., Wang, D., Cui, J. (2020). Neuroprotective effects of leptin on cerebral ischemia through JAK2/STAT3/PGC-1-mediated mitochondrial function modulation. *Brain Res Bull. 156*, pp.118-130. doi: 10.1016/j.brainresbull.2020.01.002.

Zorova, LD., Popkov, VA., Plotnikov, EY., Silachev, DN., Pevzner, IB., Jankauskas, SS., Babenko, VA., Zorov, SD., Balakireva, AV., Juhaszova, M., Sollott, SJ., Zorov, DB. (2018).

Mitochondrial membrane potential. *Anal Biochem 552*, pp. 50-59. doi: 10.1016/j.ab.2017.07.009

Acknowledgements:

I'd like to sincerely thank my supervisor, Dr Gayle Doherty, and her PhD students for all the help and support I have received over the course of my Laidlaw research. I'd also like to express my gratitude to Lord Laidlaw and the Laidlaw Foundation for this incredible opportunity to conduct the research.